Role of Acidic and Aromatic Amino Acids in *Rhodobacter Capsulatus* Cytochrome c_1. A Site-Directed Mutagenesis Study†

Jun Li,‡ Artur Osyczka,§ Richard C. Conover,|| Michael K. Johnson,|| Hong Qin,‡,⊥ Fevzi Daldal,# and David B. Knaff*,‡

Department of Chemistry and Biochemistry and Center for Biotechnology and Genomics, Texas Tech University, Lubbock, Texas 79401-1061, The Johnson Research Foundation, Department of Biochemistry and Biophysics, and Plant Science Institute, Department of Biology, University of Pennsylvania, Philadelphia, Pennsylvania 19104, and Department of Chemistry and Center for Metalloenzyme Studies, University of Georgia, Athens, Georgia 30602

Received December 10, 2002; Revised Manuscript Received May 20, 2003

ABSTRACT: The roles of two evolutionarily conserved aromatic residues in the cytochrome c_1 component of the *Rhodobacter capsulatus* cytochrome bc_1 complex, phenylalanine 138 and tyrosine 194, were analyzed by site-directed mutagenesis, in combination with biophysical and biochemical measurements. Changing Phe138 to either alanine or valine, but not to tyrosine, results in redox heterogeneity of cytochrome c_1. Replacement of Phe138 by an aliphatic amino acid also caused changes in the EPR spectrum of the cytochrome and resulted in decreases in the steady-state V_{max} for the hydroquinone/cytochrome *c* oxidoreductase activity of cytochrome bc_1 complexes containing the mutated cytochrome c_1. These findings indicate that the presence of an aromatic residue at position 138 is essential for maintaining the native environment of the cytochrome c_1 heme. In contrast, replacement of Tyr194 by aliphatic amino acids had no significant effect on either the E_m of cytochrome c_1 or the steady-state activity parameters. Site-directed mutagenesis of glutamate and aspartate residues in a conserved acidic patch (region 2) on *Rb. capsulatus* cytochrome c_1 suggests that these negatively charged residues do not play a role in the docking of cytochrome c_2 with the cytochrome bc_1 complex.

The cytochrome bc_1 complex (ubihydroquinone/cytochrome *c* oxidoreductase) plays an essential role in both photosynthetic and respiratory electron-transfer pathways (*1*−*3*). Electron transfer through the complex is coupled to proton translocation and the formation of a trans-membrane electrochemical gradient (*1*−*3*). The electrochemical gradient generated is subsequently used as an energy source for ATP synthesis by ATP synthase, for active transport, and for other energy-requiring processes. Cytochrome bc_1 complexes isolated from purple non-sulfur bacteria, such as *Rhodobacter capsulatus*, *Rb. sphaeroides*, *Rhodospirillum rubrum*, and *Rhodopseudomonas viridis*, contain only three or four subunits, while the corresponding mitochondrial complexes usually have 10 or more subunits (*4*). The simpler subunit composition of the cytochrome bc_1 complexes from these bacteria and the possibility of studying the light-driven passage of a single electron through the complexes make them excellent experimental systems for investigating the mechanism of electron transfer within the bc_1 complex and between the complex and its electron-accepting and electron-donating reaction partners.

Recently obtained crystal structures of three mitochondrial cytochrome bc_1 complexes have provided a clear picture of the quaternary structure of the complex and of the tertiary structures of individual subunits (*5*−*8*), including the three conserved, redox-active subunits responsible for the electron-transfer reactions in all cytochrome bc_1 complexes (i.e., the Rieske iron−sulfur protein, cytochrome c_1, and cytochrome *b* (*2*)). The cytochrome *b* subunit is largely embedded in the membrane and contains two noncovalently bound hemes (high- and low-potential protohemes, designated as b_H and b_L, respectively). The cytochrome c_1 subunit has an extrinsic hydrophilic domain, with a single covalently bound *c*-type heme, and a C-terminal hydrophobic α-helical transmembrane anchor. The Rieske iron−sulfur protein subunit contains a bulky hydrophilic domain with a single [2Fe−2S] cluster and an N-terminal hydrophobic membrane anchor. A large domain movement involving a portion of the Rieske protein has been proposed, based on the crystal structures of the mitochondrial cytochrome bc_1 complexes with different bound inhibitors (*7*), and substantial evidence supporting this hypothesis has been obtained (*3*). The X-ray structures have also provided strong supporting evidence for models of the complex that had been proposed as a result of earlier biochemical, biophysical, and genetic studies (*9*).

† Supported by grants from the Robert A. Welch Foundation (D-0710 to D.B.K.), the National Institutes of Health (GM38237 to F.D., GM62524 to M.K.J., and GM27309 to P. Leslie Dutton), and the National Science Foundation (MCB-9808857 to M.K.J.).

* To whom correspondence should be addressed. Phone: (806) 742-0288. Fax: (806) 742-2025. E-mail: Knaff@ttu.edu.

‡ Texas Tech University.

§ The Johnson Research Foundation, Department of Biochemistry and Biophysics, University of Pennsylvania.

|| University of Georgia.

⊥ Current address: Bayer Corporation, 400 Morgan Lane, West Haven, CT 06516.

Plant Science Institute, Department of Biology, University of Pennsylvania.

10.1021/bi020693r CCC: $25.00
Published on Web 06/25/2003

Table 1: Sequence Alignment of Cytochrome c_1 from Chicken, Beef, Yeast, *Rb. capsulatus*, and *Rb. sphaeroides*

region 1	chicken	(62)[a]	KALAEEVEVQDGPNEDGEMFMRPGKLSDY
	beef	(62)	KALAEEVEVQDGPNEDGEMFMRPGKLSDY
	yeast	(126)	RNMAEEFEYDDEPDEQGNPKKRPGKLSDY
	Rb. capsulatus	(59)	TFVREYAAGLDTIIDKDSGEERDRKETDM
	Rb. sphaeroides	(61)	DQVRAYAT-QFTVTDEETGEDREGKPTDH
region 2	chicken	(165)	YNDVLE**F**DDGTPA
	beef	(165)	NEVLE**F**DDGTPA
	yeast	(230)	FDDMVE**Y**EDGTPA
	Rb. capsulatus	(188)	VDDQVT**Y**EDGTPA
	Rb. sphaeroides	(190)	MDDLVE**Y**ADGHDA
region 3	chicken	(132)	TG**Y**CE-PPT- -GVSVREG
	beef	(132)	TG**Y**CE-PPT- -GVSLREG
	yeast	(196)	TG**Y**PDEPPA- -GVALPPG
	Rb. capsulatus:	(136)	IG**F**EENPE- -CAPEGIDG
	Rb. sphaeroides:	(136)	TG**F**PEEPPKCAEGHEPDG

[a] The starting position of each sequence is indicated for comparison. For *Rb. capsulatus* and *Rb. sphaeroides*, the numbering system is based on the mature forms of the proteins. The sequence of the precursor form of yeast cytochrome c_1 has been used for its numbering, to facilitate direct comparison with the recently published cocrystal structure of yeast cytochrome bc_1 complex and iso-1-cytochrome *c* (*29*). The conserved aromatic residues are shown in bold, and the conserved acidic residues are underlined.

The electron-transfer reactions and the coupled proton translocation associated with the cytochrome bc_1 complex are best described by a bifurcated Q-cycle mechanism (*2*, *10*, *11*). One of the two electrons generated through oxidation of hydroquinone (QH_2)[1] at the Q_o site goes through a low-potential chain (i.e., from the b_H heme to the b_L heme) and reduces quinone (Q) bound at the Q_i site. The other electron is transferred through a high-potential chain composed of the Rieske protein and cytochrome c_1. This electron leaves the complex when the heme of cytochrome c_1 reduces one of a number of possible electron acceptors, such as cytochrome *c* in mitochondria and aerobic prokaryotes (*1*−*3*, *11*), and either the soluble proteins, cytochrome c_2, cytochrome c_8, and high-potential iron−sulfur protein (HiPIP) or the membrane-bound cytochrome c_y in anoxygenic photosynthetic bacteria (*12*−*14*).

Chemical modification and site-directed mutagenesis studies have identified several conserved lysine residues surrounding the exposed heme edge on the surface of cytochrome c_2 that are involved in binding this electron acceptor for the bacterial cytochrome bc_1 complex to cytochrome c_1 (*15*−*20*). Differential chemical labeling of mitochondrial cytochrome c_1 in the presence and absence of cytochrome *c* (*21*) and photoaffinity cross-linking of mitochondrial cytochrome c_1 to cytochrome *c* (*22*) implicated two acidic regions on cytochrome c_1, referred to as region 1 and region 2 (Figure 1), in the binding of cytochrome *c*. A site-directed mutagenesis study of the interaction of cytochrome c_1 in the cytochrome bc_1 complex of *Rb. sphaeroides*, which closely resembles the cytochrome bc_1 complex of *Rb. capsulatus*, with cytochrome *c* (*23*), implicated a third acidic region on cytochrome c_1, referred to as region 3 (Figure 1), as a possible binding site for cytochrome c/c_2. Although region 2 is the best-conserved of these three acidic regions on cytochrome c_1 (see Table 1), site-directed mutagenesis studies with *Rb. sphaeroides* cytochrome c_1 suggested that acidic amino acids in this region are not involved in binding cytochrome c/c_2 (*23*). While a recent X-ray structure for the complex formed between the yeast cytochrome bc_1 complex and its electron acceptor, iso-1-cytochrome *c* (*24*), does support the idea that region 2 of cytochrome c_1 is involved in binding cytochrome *c*, the binding interactions are largely hydrophobic rather than electrostatic in nature.

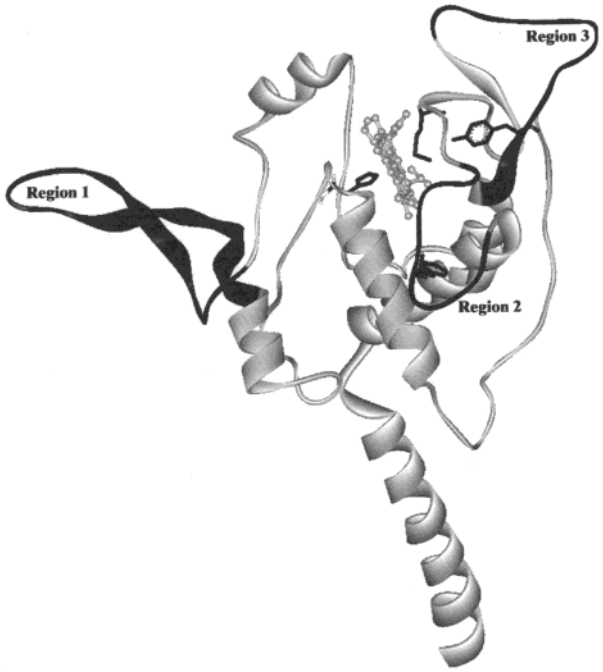

FIGURE 1: Crystal structure of chicken cytochrome c_1, showing possible cytochrome *c*-binding regions. Three possible binding sites for cytochrome *c* are shown in dark black ribbons. The heme axial ligands, H41 and M160 (corresponding to H38 and M183 in *Rb. capsulatus* cytochrome c_1), and two conserved aromatic amino acid residues, one in region 2 (F171, corresponding to Y194 in *Rb. capsulatus* cytochrome c_1) and one in region 3 (Y134, corresponding to F138 in *Rb. capsulatus* cytochrome c_1), are shown as stick models in dark black. The heme is shown, in gray, as a stick model. Twenty-one residues of the C-terminal membrane-anchoring portion of the cytochrome, running from Y221 to K241, were truncated to show the heme environment more clearly. The structure is adapted from that presented in ref *7*.

[1] Abbreviations: DAD, 2,3,5,6-tetramethyl-1,4-phenylenediamine; DBH_2, 2,3-dimethoxy-5-decyl-6-methyl-1,4-benzohydroquinone; EPR, electron paramagnetic resonance; E_h, ambient potential; E_m, redox midpoint potential; E_{m7}, redox midpoint potential at pH 7; HiPIP, high-potential iron−sulfur protein; MOPS, 3-(*N*-morpholino)propanesulfonic acid; MPYE, magnesium−calcium peptone yeast extract; PES, *N*-ethyldibenzopyrazine ethosulfate; PMS, *N*-methyl-dibenzopyrazine methosulfate; Q and QH_2, oxidized and reduced ubihydroquinone, respectively; Q_o and Q_i, QH_2 oxidation site and Q reduction site, respectively; SDS−PAGE, polyacrylamide gel electrophoresis in the presence of sodium dodecyl sulfate; Tris, tris(hydroxymethyl)aminomethane.

Table 2: Oligonucleotides Used for Site-Directed Mutagenesis (F and R denote Forward and Reverse Primers, Respectively)[a]

Y194A(F)	5′-TGGTGGATGATCAGGTCACCGCCGAGGACGGCACCCCGGCCA-3′
Y194F(F)	5′-GATCAGGTCACCTTCGAGGACGGCACC-3′
Y194V(F)	5′-GATCAGGTCACCGTCGAGGACGGCACC-3′
E195K(R)	3′-CCAGTGGATGTTCCTGCCGTGGGGC-5′
E195Q(F)	5′-GGTCACCTACCAGGACGGC-3′
D196K(F)	5′-CAGGTCACCTACGAGAAAGGCACCCCGGCCACC-3′
D189N/D190N(F)	5′-GCCGCTGGTGAATAATCAGGTCACCTACGAGGACGGCACCCCG-3′
D189E/D190E/D196E(F)	5′-GCCGCTGGTGGAGGAGCAGGTCACCTACGAGGAAGGCACCCCG-3′
D189K/D190K/D196K(F)	5′-GCCGCTGGTGAAGAAGCAGGTCACCTACGAGAAAGGCACCCCG-3′
D189N/D190N/D196N(F)	5′-GCCGCTGGTGAATAATCAGGTCACCTACGAGAACGGCACCCCG-3′
F138A(F)	5′-CATCTACAACTACGTCATCGGTGCCGAAGAAAACCCGGAATGC-3′
F138A(R)	3′-GCATTCCGGGTTTTCTTCGGCACCGATGACGTAGTTGTAGATG-5′
F138V(F)	5′-CAACTACGTCATCGGTGTCGAAGAAAACCCGGAATG-3′
F138V(R)	3′-CATTCCGGGTTTTCTTCGACACCGATGACGTAGTTG-5′
F138Y(F)	5′-CAACTACGTCATCGGTTACGAAGAAAACCCGGAATG-3′
F138Y(R)	3′-CATTCCGGGTTTTCTTCGACACCGATGACGTAGTTG-5′

[a] The underlined bases correspond to the genetic codes for the amino acid(s) to be mutated.

We have undertaken extensive characterization of a large number of charge-elimination and charge-reversal site-directed variants in region 2 of *Rb. capsulatus* cytochrome c_1, in an attempt to further elucidate a possible role for acidic residues in region 2 in binding the electron-accepting substrate for the cytochrome bc_1 complex. As both region 2 and 3 each contain one highly conserved aromatic residue (see Table 1) and such residues have been implicated as facilitators of electron-transfer reactions in some heme-containing proteins (*25*−*31*), the mutagenesis study was extended to explore possible roles for these two aromatic amino acids in the function of *Rb. capsulatus* cytochrome c_1. The results of this study suggest that the conserved aromatic residue in region 3, Phe138, plays an important role in stabilizing the native heme environment of *Rb. capsulatus* cytochrome c_1.

MATERIALS AND METHODS

Initial mutagenesis with the pPET1 plasmid (containing a wild-type copy of *pet*ABC, which encodes Rieske protein, cytochrome *b*, and cytochrome c_1) as the template (*32*) was accomplished using either the Transformer site-directed mutagenesis kit from CLONTECH or the QuickChange from Stratagene. All the primers (Table 2) were synthesized on a Beckman Oligo 1000M DNA Synthesizer in the Core Facility of the Texas Tech University Center for Biotechnology and Genomics. After sequencing confirmed that the desired base changes had been made and that no other base changes had occurred, the mutated pPET1 plasmid was ligated to the broad-range host plasmid pRK404 and was introduced into a *pet*ABC deletion strain, *Rb. capsulatus*, MT-RBC1, via tri-parental crosses as described previously (*32*). The efficacies of the mutagenesis procedures were confirmed by sequencing plasmids isolated from the appropriate *Rb. capsulatus* transconjugants.

Respiratory growth of *Rb. capsulatus* strains in MPYE (magnesium−calcium peptone yeast extract) medium was achieved at 35 °C in the dark with moderate shaking (60−100 rpm). Photosynthetic growth of *Rb. capsulatus* at room temperature (22−25 °C) under continuous light and anaerobic conditions was carried out on MPYE plates containing appropriate antibiotics. Preparation of chromatophores and purification of the cytochrome bc_1 complexes were performed as described previously (*33*, *34*). Cytochrome bc_1 complex-containing fractions were pooled and analyzed for purity by SDS−PAGE (performed using a Pharmacia PhastGel system) and by absorbance spectra, and then aliquots (0.5−1.0 mL) of purified complex were stored at −80 °C in 100 mM Tris-HCl buffer (pH 8.0) containing 50 mM NaCl and 0.01% dodecyl maltoside.

Spectra of oxidized and reduced samples were recorded with a Shimadzu Model UV-2100 spectrophotometer at 1 nm spectral resolution. The spectra of ferricyanide-oxidized samples were recorded after adding 3 μL of 0.1 M potassium ferricyanide to both the sample cuvette, containing 1 mL of the cytochrome bc_1 complex, and to the reference cuvette, containing 1 mL of the sample buffer (50 mM Tris-HCl, pH 8.0, containing 100 mM NaCl and 0.01% dodecyl maltoside) but no cytochrome bc_1 complex. Spectra of ascorbate-reduced samples were recorded in a similar way, but using freshly prepared 0.1 M sodium ascorbate as a reductant instead of potassium ferricyanide as an oxidant. Spectra of dithionite-reduced samples were recorded after the addition of small amounts of solid sodium dithionite. Redox difference spectra in the α-band region were obtained by computer subtraction of a spectrum of an oxidized sample from the spectrum of a reduced sample of equal cytochrome bc_1 complex concentration. As the ferricyanide anion has a broad peak, centered at 420 nm, redox difference spectra in the Soret band region required an additional step, in which Bio-Spin 30 Columns (BIO-RAD) were used to remove the ferricyanide before spectra were recorded. The concentration of the cytochrome bc_1 complexes were based on the amount of cytochrome c_1 present, as determined by pyridine hemochromogen method (*35*).

Redox titrations of chromatophores or of purified cytochrome bc_1 complexes were carried out as described by Dutton (*36*). The cytochrome bc_1 complex (1−2 mg) was diluted to 9 mL with 50 mM MOPS buffer (pH 7.0) containing 100 mM KCl, 0.01% dodecyl maltoside, and the following redox mediators, all at a concentration of 25 μM: 1,1′-dimethylferrocene, 1,4-benzoquinone, 1,2-naphthoquinone, PMS, PES, menadione, 2-hydroxy-1,4-naphthoquinone, and anthraquinone-2-sulfonic acid. For redox difference spectra involving samples poised at $E_h = -430$ mV, 10 μM methyl viologen was also present. The titrations shown below, which were carried out in the oxidative direction, were performed by first oxidizing the sample to $E_h = +400$ to +450 mV with 0.1 M potassium ferricyanide and then reducing it by stepwise additions of 0.1 M sodium dithionite

in 0.3 M sodium bicarbonate. Titrations were also carried out in the reverse oxidative direction, and no significant differences were observed between these titrations and the titrations carried out in the reductive direction. E_m values were determined by fitting the data to the Nernst equation for a one-electron carrier ($n = 1$) with one component using Microsoft Excel.

The steady-state 2,3-dimethoxy-5-decyl-6-methyl-1,4-benzohydroquinone (DBH_2)/cytochrome *c* oxidoreductase activity of the purified bc_1 complex was assayed by following the absorbance increase at 550 nm because of the reduction of cytochrome *c*, as described previously (*20*, *37*) using an extinction coefficient of 20 mM^{-1} cm^{-1} for equine cytochrome *c* at 550 nm. The reaction was initiated by adding 5 μL of 20 mM DBH_2 (to give a final DBH_2 concentration of 0.1 mM) to 1 mL of oxidized horse heart cytochrome *c* in 50 mM potassium phosphate buffer (pH 7.4) containing 0.3 mM EDTA. Cytochrome *c* concentrations ranged from 0.8 to 50 μM. The initial slow absorbance change arising from the nonenzymatic reduction of cytochrome *c* by DBH_2 was recorded. Monitoring of the absorbance at 550 nm was continued, after 3 μL of cytochrome bc_1 complex stock solution (2−5 μM) was added to initiate cytochrome bc_1-catalyzed electron transfer from DBH_2 to cytochrome *c*. The initial enzymatic reaction rate was calculated by subtracting the nonenzymatic rate from the enzymatic rate. The steady-state parameters V_{max} and K_m were determined from Eadie−Hofstee plots of the initial rates v versus v/[S], where [S] is the concentration of cytochrome *c*. Microsoft Excel was used to calculate V_{max} and K_m from the Eadie−Hofstee plots.

Flash-induced kinetic measurements of *c*-type cytochromes in freshly prepared chromatophores were carried out as described previously (*33*, *38*). The measurements were performed in 50 mM MOPS buffer (pH 7.0) containing 100 mM KCl, 2.5 μM valinomycin, and appropriate redox mediators (*33*). The samples were poised at an ambient redox potential of +100 mV. Under these conditions, the ubiquinone pool is partially reduced, and all the high-potential components of the cytochrome bc_1 complex are reduced before flash activation. The concentrations of chromatophores were adjusted so that all samples contained 0.25 μM reaction center. Reaction center concentrations were estimated, using a reduced minus oxidized extinction coefficient of 29 mM^{-1} cm^{-1} (*39*), from the magnitude of the absorbance decrease at 602 minus 540 nm caused by a train of 10 flashes spaced 20 ms apart using samples poised at an ambient potential of +380 mV (*33*). At this E_h value, all of the in situ electron donors to the reaction center are oxidized prior to the flash, preventing any rapid reduction of the photooxidized reaction center. The train of 10 flashes saturates the absorbance decrease, ensuring that the reaction center is fully oxidized.

X-band EPR studies of purified cytochrome bc_1 complexes were carried out using a Bruker ESP-300E spectrometer equipped with an Oxford Instruments ESR-9 flow cryostat, as described previously (*40*). Spectral simulations were carried out using the Simfonia software package (Bruker Instruments). Spin quantitations of high-spin components were carried out under nonsaturating conditions, using the resonance arising from reduced Rieske center in dithionite-reduced samples as an internal standard, following the protocols developed by Aasa and Vänngård (*41*).

Table 3: Photosynthetic Growth of Different *Rb. capsulatus* Strains and Heme-Contents and Steady-State Kinetic Parameters for Purified Cytochrome bc_1 Complexes Isolated from These Strains[a]

strain	PS growth	protoheme/ mesoheme[b]	K_m (μM^{-1})	V_{max} (s^{-1})
wild type	++	1.65 ± 0.02	5.4 ± 0.16	32.4 ± 0.8
D189N/D190N	++	1.70 ± 0.01	10.37 ± 0.16	30.6 ± 0.1
D189E/D190E/D196E	++	1.46 ± 0.00	7.40 ± 0.52	10.8 ± 0.4
D189N/D190N/D196N	++	1.71 ± 0.01	8.20 ± 0.01	25.5 ± 0.6
D189K/D190K/D196K	++	2.02 ± 0.07	17.64 ± 0.89	18.2 ± 0.0
E195Q	++	1.50 ± 0.03	6.88 ± 0.63	21.7 ± 0.0
E195K	++	1.52 ± 0.21	8.08 ± 0.22	20.8 ± 0.3
D196K	++	1.67 ± 0.02	5.46 ± 0.08	19.8 ± 0.4
Y194A	++	1.79 ± 0.02	5.42 ± 0.26	20.0 ± 0.1
Y194V	++	1.90 ± 0.02	6.35 ± 0.13	20.0 ± 0.4
Y194F	++	1.63 ± 0.03	7.02 ± 0.39	23.8 ± 1.7
F138A	++	1.87 ± 0.02	4.74 ± 0.04	5.1 ± 0.1
F138V	++	1.84 ± 0.02	5.30 ± 0.14	16.0 ± 0.6
F138Y	++	1.66 ± 0.08	7.48 ± 0.35	17.7 ± 0.2

[a] All data were expressed as mean ± SD (standard deviation) averaged from several experiments ($n = 3$ for hemochromogen assays and $n = 2$ for the steady-state kinetic measurements). PS refers to photosynthetic, and the strains are identified by the substitutions made in the cytochrome c_1 subunit of the cytochrome bc_1 complexes present in these strains. [b] Protoheme/mesoheme ratios (i.e., cytochrome *b* heme/cytochrome c_1 heme) were calculated from dithionite minus ferricyanide redox difference spectra obtained using the pyridine hemochromogen method (*25*).

RESULTS

Photosynthetic Growth, Composition, and α-Band Absorbance Spectra. All of the *Rb. capsulatus* strains containing the mutations in the cytochrome c_1 subunit of the cytochrome bc_1 complexes that were produced during this study were capable of growing photosynthetically under anaerobic conditions with growth rates similar to that of the wild-type strain (Table 3). It can thus be concluded that none of these mutations inhibited electron flow through the cytochrome bc_1 complex to an extent sufficient to significantly impair photosynthetic growth.

All of the purified cytochrome bc_1 complexes produced for this study exhibited Coomassie Blue-staining patterns, after gel electrophoresis under denaturing conditions (SDS−PAGE), that were similar to that observed with the wild-type cytochrome bc_1 complex (i.e., showing three major bands arising from cytochrome *b*, cytochrome c_1, and the Rieske protein (not shown)). Pyridine hemochromogen analyses of the wild-type and cytochrome c_1 variants of the *Rb. capsulatus* cytochrome bc_1 complexes gave ratios of protoheme/mesoheme close to the stoichiometric ratio of 2:1 predicted for a complex with a mono-heme *c*-type cytochrome and a di-heme *b*-type cytochrome (Table 3). For the wild-type cytochrome bc_1 complex, the ratio of protoheme/mesoheme obtained (1.65:1) agrees, within the experimental uncertainties of the measurement, with previously reported ratios ranging from 1.7:1 to 1.75:1 (*33*, *42*). The values measured for the wild-type complex in these studies may differ from the 2:1 value expected from the known structure of the complex either because recovery of noncovalently bound protoheme can be less than 100% (*35*) and/or because the purified complexes contain small amounts of *c*-type cytochrome impurities (other than cytochrome c_1) that were not detected in reduced minus oxidized difference spectra or by SDS−PAGE (*34*).

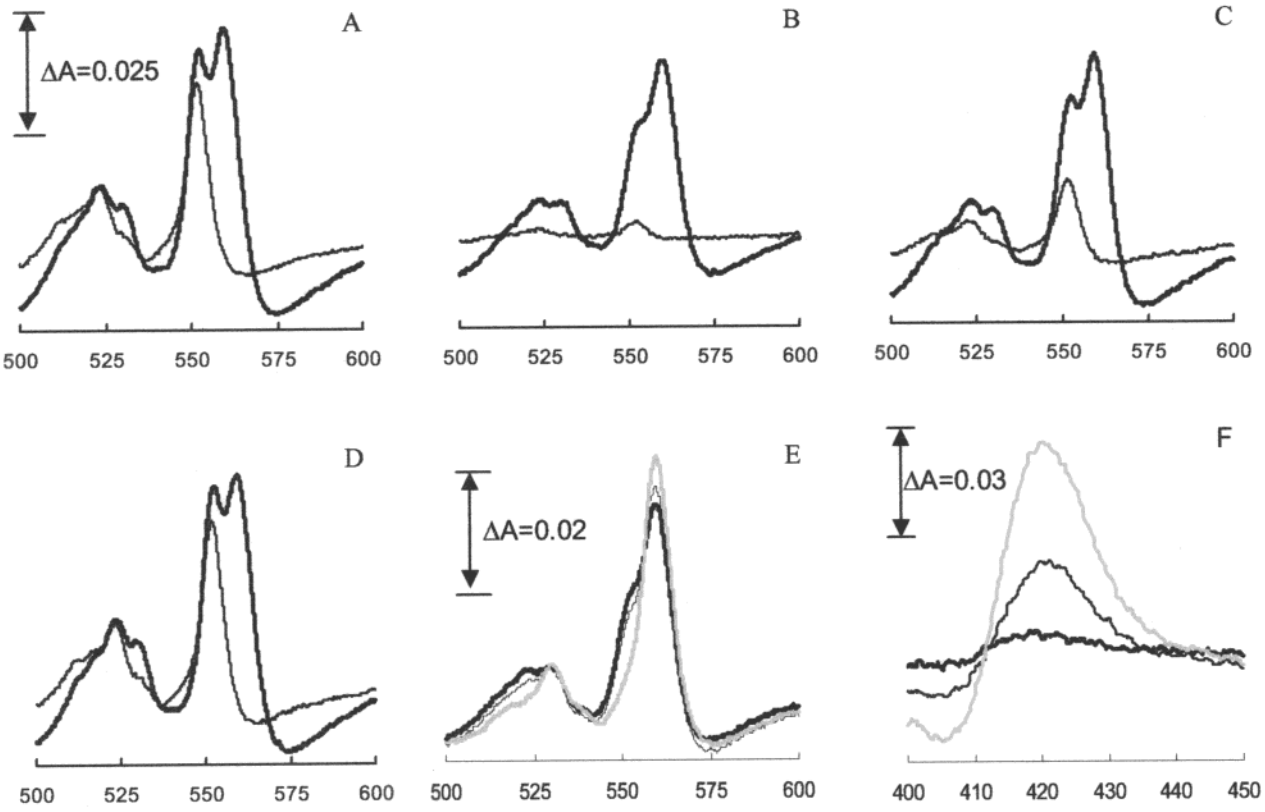

FIGURE 2: Reduced minus oxidized difference spectra of *Rb. capsulatus* cytochrome bc_1 complexes. For panels A−D, taken in the α- and β-band spectral region, purified cytochrome bc_1 complexes, at a concentration of 2 μM, were dissolved in 50 mM Tris-HCl buffer (pH 8.0) containing 100 mM NaCl and 0.01% dodecyl maltoside. The dark lines represent dithionite-reduced minus ferricyanide-oxidized difference spectra, and the light lines represent ascorbate-reduced minus ferricyanide-oxidized spectra. (A) Wild type; (B) F138A; (C) F138V; and (D) F138Y. The absorbance scale is the same for panels A−D. Panel E shows dithionite minus ascorbate difference spectra for cytochrome bc_1 complexes containing the F138Y (gray trace), F138V (thin black trace), and F138A (thick black trace) variants of cytochrome c_1, obtained by computer subtraction of the (ascorbate minus ferricyanide) difference spectra from (dithionite minus ferricyanide) difference spectra shown in panels B−D. Conditions for panel F, taken in the Soret-band region, were identical to those used for obtaining the ascorbate minus ferricyanide difference spectra of panels A−D, except that the cytochrome bc_1 complexes were present at a concentration of 1 μM and had been pretreated with ferricyanide and the ferricyanide then removed, as described in Materials and Methods. The upper trace (shown in gray) was obtained with the F138Y variant of cytochrome c_1, the middle trace (shown as a thin black line) with the F138V variant, and the lower trace (shown as a thick black line) with the F138A variant.

For all the cytochrome bc_1 complexes studied in this work, difference spectra of ascorbate-reduced minus ferricyanide-oxidized samples exhibited an α- and a β-band, with maxima at 551−552 and 523−524 nm, respectively. (Under the conditions used to obtain these spectra, the addition of ascorbate produced no detectable reduction of either cytochromes b_L or b_H. Thus, these α- and β-bands can be attributed solely to reduced cytochrome c_1.) However, the magnitudes of the cytochrome c_1 α- and β-bands for cytochrome bc_1 complexes containing either the F138A and the F138V variants of cytochrome c_1 are considerably smaller in ascorbate-reduced minus ferricyanide-oxidized difference spectra than those observed with an equal concentration of wild-type cytochrome bc_1 complex (Figure 2A−C). The decrease in α-band magnitude in an ascorbate-reduced sample is particularly noticeable for the F138A variant. In contrast, ascorbate-reduced samples of the cytochrome bc_1 complex containing the F138Y variant of cytochrome c_1 (Figure 2D) showed α- and β-bands with magnitudes very similar to those of the wild-type cytochrome. The addition of *N*-methyl-dibenzopyrazine methosulfate (PMS), an excellent redox mediator for *c*-type cytochromes (*36*), to ascorbate-reduced samples produced no increase in the magnitude of the peak at 552 nm arising from reduced cytochrome c_1 (data not shown). Dithionite minus ascorbate difference spectra of cytochrome bc_1 complexes containing either the F138V or the F138A variant of cytochrome c_1 (Figure 2E) clearly indicate, as shown by the presence of a distinct shoulder at 552 nm, that a considerable portion of the F138A and F138V cytochrome c_1 variants is reducible by dithionite but not by ascorbate. In contrast, dithionite minus ascorbate difference spectra for cytochrome bc_1 complexes containing either wild-type cytochrome c_1 (not shown) or its F138Y variant (Figure 2E) show only features attributable to cytochromes b_H and b_L, indicating that wild-type cytochrome c_1 and its F138Y variant are both completely reducible by ascorbate. The pattern of low-amplitude changes in cytochrome spectra, on the addition of ascorbate as a reductant, for the F138V and particularly for the F138A variant of cytochrome c_1, can also be seen in ascorbate minus ferricyanide redox difference spectra in the Soret-band region (Figure 2F), when compared to the spectra obtained with a cytochrome bc_1 complex containing either the F138Y variant of cytochrome c_1 (Figure 2F) or the wild-type cytochrome c_1 (not shown).

No decrease in α-band intensity (as compared to that observed for wild-type cytochrome c_1) was observed in spectra of ascorbate-reduced samples of any of the region 2

Table 4: Steady-State DBH_2: Cytochrome *c* Activity and Cytochrome c_1 Midpoint Potentials[a]

	chromatophore		purified bc_1 complex	
strain	activity	$E_{m,7}$ (mV)	activity	$E_{m,7}$ (mV)
WT	100.0	$+320 \pm 7$ ($n = 4$)	100.0	$+329 \pm 5$ ($n = 7$)
D189N/D190N	nd	nd	94.4	$+332 \pm 1$ ($n = 2$)
D189K/D190K/D196K	nd	nd	56.2	$+334 \pm 1$ ($n = 2$)
Y194A	nd	nd	61.7	$+333 \pm 1$ ($n = 2$)
Y194V	nd	nd	61.7	$+335 \pm 8$ ($n = 3$)
F138A	17.6	$+226 \pm 13$ ($n = 3$)	15.7	$+219 \pm 3$ ($n = 2$)
F138V	57.9	$+247 \pm 7$ ($n = 4$)	49.4	$+242 \pm 3$ ($n = 2$)
F138Y	86.2	$+292 \pm 2$ ($n = 2$)	54.6	$+296 \pm 6$ ($n = 3$)

[a] For chromatophores, the activity was determined using 100 μM horse cytochrome *c*, and for purified cytochrome bc_1 complexes, the relative activities were calculated from the V_{max} values listed in Table 3. The activities, in both cases, are expressed as percentages of the activity obtained with samples containing wild-type cytochrome c_1. (The 100% wild type level corresponds to 3.25 μmol of cytochrome *c* reduced per min per mg of protein for chromatophores and 32.4 μmol of cytochrome *c* reduced per s per μmol of cytochrome bc_1 complex for the purified complex.) Data are expressed as mean $\pm$ SD; *n* is the number of determinations, and nd indicates not determined.

variants generated for this study (not shown). Of particular interest was the observation that, in contrast to the effects on the ascorbate-reducibility produced by mutating F138 to a nonaromatic amino acid, ascorbate-reduced samples of *Rb. capsulatus* cytochrome bc_1 complexes containing the Y194A or Y194V variants of cytochrome c_1 exhibit α-bands with maxima at 552 nm and the same amplitude as that observed for the wild-type cytochrome (Y194 is another well-conserved aromatic residue in cytochrome c_1—see Table 1).

Oxidation−Reduction Potentials. To characterize the redox properties of the three position 138 variants of cytochrome c_1 further, oxidation−reduction titrations of the F138A, F138V, and F138Y variants were carried out and compared to titrations of the wild-type cytochrome. Oxidation−reduction titrations (not shown) of the wild-type cytochrome c_1, in chromatophore membranes or in purified cytochrome bc_1 complexes, gave E_m values of $+320 \pm 7$ and $+329 \pm 5$ mV, respectively (Table 4). Chromatophore membranes contain several high-potential *c*-type cytochromes with similar α-band absorbance maxima (*42*); thus, E_m values determined from measurements using these membranes may not in general reflect E_m values for cytochrome c_1 as accurately as will be the case for measurements made with purified cytochrome bc_1 complexes. Nevertheless, the fact that E_m values obtained using chromatophores are so similar to those obtained using purified cytochrome bc_1 complexes, both for samples containing either wild-type cytochrome c_1 or several site-specific variants (see below), led us to tentatively attribute the $E_m = +329$ mV component in *Rb. capsulatus* chromatophores to wild-type cytochrome c_1. The E_m value obtained for *Rb. capsulatus* cytochrome c_1 in the purified cytochrome bc_1 complex is in good agreement with recently published values (*38*, *43*). Figure 3A shows titration data obtained with a sample of purified cytochrome bc_1 complex containing the F138A variant of cytochrome c_1. The data give an excellent fit to the Nernst equation for a single $n = 1$ component with a midpoint potential of +216 mV. The average E_m value obtained for this variant in purified cytochrome bc_1 complexes, $+219 \pm 3$ mV (Table 4), is significantly lower (ca. 110 mV) than that observed for the wild-type cytochrome c_1 in samples of the purified cytochrome bc_1 complex. A very similar E_m value, $+226 \pm 13$ mV, was obtained for the component with an α-band maximum at 552 nm observed in titrations of chromatophore membranes containing the F138A variant of cytochrome c_1 (Table 4). Figure 3C shows that replacing Phe138 by another aliphatic amino acid, valine, also lowers the E_m of *Rb. capsulatus* cytochrome c_1 significantly from that of the wild-type cytochrome. The data again give an excellent fit to the Nernst equation for a single $n = 1$ component, in this case with $E_m = +239$ mV, for the F138V variant of cytochrome c_1. Average E_m values measured for the component with an α-band maximum at 552 nm in chromatophore membranes ($+247 \pm 7$ mV) and in purified cytochrome bc_1 complexes ($+242 \pm 3$ mV) containing the F138V variant of cytochrome c_1 agree well with each other (Table 4) and are ca. 90 mV lower than values measured for the wild-type cytochrome. Figure 3E shows the results of a titration of purified cytochrome bc_1 complex containing the F138Y variant of cytochrome c_1. The data give an excellent fit to the Nernst equation for a single $n = 1$ component with $E_m = +298$ mV. Average E_m values determined for the F138Y variant in purified cytochrome bc_1 complexes ($E_m = +296 \pm 6$ mV) and in chromatophore membranes ($E_m = +292 \pm 2$ mV) were similar (Table 4). The fact that the decrease in the E_m value of *Rb. capsulatus* cytochrome c_1 of ca. 30 mV, as compared to the wild-type cytochrome, produced by a Phe/Tyr substitution is considerably smaller than the ca. 100 mV shift observed with the F138A and F138V variants is not surprising in view of the conservative replacement of one aromatic amino acid by another. The observation that essentially identical changes in E_m, caused by replacement of F138, are observed in chromatophores and in purified cytochrome bc_1 complexes suggest that these changes are not related to a decrease in the stability of the complex during purification that arises from replacement of F138 by a nonaromatic amino acid.

When redox titrations of purified cytochrome bc_1 complexes were extended to more negative ambient potential values (i.e., $E_h = -250$ mV), the E_m values measured for cytochromes b_H and b_L in cytochrome bc_1 complexes containing either F138A, F138V, or F138Y variants of cytochrome c_1 were identical to those observed for the complex containing wild-type cytochrome c_1 (data not shown). Thus, the effects of replacing Phe138 of cytochrome c_1 on heme redox potentials are confined to the cytochrome c_1 subunit.

Difference spectra recorded during the titration of the cytochrome bc_1 complex containing the F138A variant of cytochrome c_1 (Figure 3B) show that only cytochrome c_1

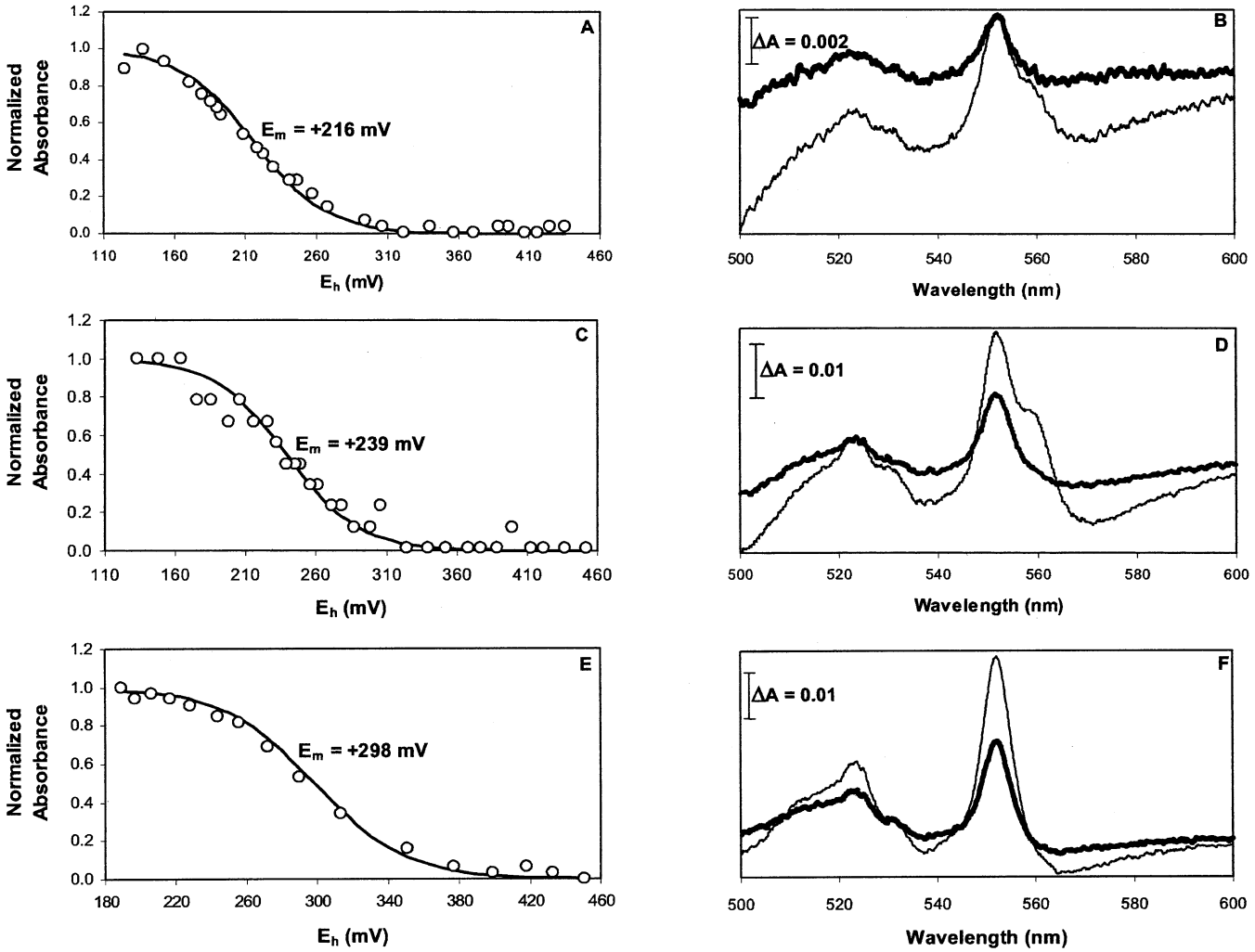

FIGURE 3: Redox titrations and redox difference spectra of three F138 variants of *Rb. capsulatus* cytochrome c_1. Cytochrome bc_1 complexes, at a concentration of 6.3 μM for the F138A variant, 3.2 μM for the F138V variant, and 2.1 μM for the F138Y variant, were present in the same buffer used to obtain the spectra of Figure 2. For the titrations shown in panels A (F138A), C (F138V), and E (F138Y), the open circles represent the actual data points, and the solid lines represent the best fit to the Nernst equation for one $n = 1$ component. For all three of these titrations, the *Y* axis amplitudes measured at each E_h value have been normalized, with the value for the fully oxidized cytochrome having been set at 0.0 and for the fully reduced cytochrome having been set at 1.0, in each case. For the titrations of panels A and C, absorbance at 550 nm was used to monitor the extent of cytochrome c_1 reduction, to minimize contributions from cytochrome b_H. However, because of the larger difference in the E_m value between F138Y cytochromes c_1 and b_H, 552 nm was used to monitor the extent of cytochrome c_1 in the titration of panel E. In the difference spectra for F138A (B), the dark trace represents a redox difference spectrum for (+218 mV) − (+322 mV), and the light trace represents a redox difference spectrum for (+138 mV) − (+322 mV). In the difference spectra for F138V (D), the dark trace represents a redox difference spectrum for (+239 mV) − (+340 mV), and the light trace represents a redox difference spectrum for (+133 mV) − (+340 mV). In the difference spectra for F138Y (F), the dark trace represents a redox difference spectrum for (+290mV) − (+399 mV), and the light trace represents a redox difference spectrum for (+189 mV) − (+399 mV).

contributes to the absorbance changes as E_h is lowered from +322 to +218 mV. The absorbance maxima in difference spectra taken between any two E_h values in this range were all centered at 551−552 nm, characteristic of the α-band of cytochrome c_1. When the ambient potential was decreased to ca. +130 mV, absorbance contributions from a *b*-type cytochrome can be detected, as demonstrated by a small shoulder at 560 nm in this difference spectrum (Figure 3B). This observation suggests that either a small amount of cytochrome b_H (E_m = +40 mV, ref *43*) is reduced or that a small amount of cytochrome *b*150 (*44*) is present in the purified cytochrome bc_1 complex used for these measurements. Similar redox difference spectra were obtained from titrations of cytochrome bc_1 complexes containing the F138V variant of cytochrome c_1 (Figure 3D) or the F138Y variant of cytochrome c_1 (Figure 3F).

It should be pointed out that the difference spectra of Figure 3B,D,F were measured using different concentrations of cytochrome bc_1 complexes (i.e., 6.3 μM for the complex containing the F138A variant of cytochrome c_1, 3.2 μM for the F138V variant, and 2.1 μM for the F138Y variant). Thus, the actual magnitude of the cytochrome c_1 α-bands observed in difference spectra obtained from these titrations was greatest for the F138Y variant and smallest for the F138A variant, with that for the F138V variant falling in the middle. In fact, the relative magnitudes of the α-bands observed for the three cytochrome c_1 variants in these titrations of purified cytochrome bc_1 complexes are quite similar to those found in the ascorbate minus ferricyanide difference spectra shown in Figure 2. Therefore, it seemed possible that the E_m = ca. +220 mV and E_m = ca. +240 mV species detected in titrations of F138A cytochrome c_1 and F138V cytochrome

c_1, respectively, might represent only one component of heterogeneous populations present in these two variants. In an attempt to detect forms of the F138A and F138V variants of cytochrome c_1, different from those detected in the redox titrations of Figure 3, that could not be reduced by ascorbate but were dithionite-reducible, difference spectra of cytochrome bc_1 complexes containing either the F138A or the F138V variant of cytochrome c_1, in which a spectrum obtained at $E_h = -220$ mV was subtracted from one obtained at $E_h = -430$ mV, were measured (cytochromes b_H and b_L are fully reduced at both ambient potentials and so would not be expected to contribute any features to these difference spectra). These difference spectra (not shown) contained no peak at or near 552 nm (in fact, these spectra were completely featureless over the entire α-band and β-band spectral regions), indicating that no cytochrome c_1 species becomes reduced over this E_h range. Thus, if F138A or F138V cytochrome c_1 components with E_m values more negative than the values near +220 and +240 mV detected in the titrations of Figure 3 do in fact exist, they must have E_m values either more negative than ca. −480 mV or more positive than ca. −170 mV. As E_h values significantly more negative than −430 mV could not be obtained at pH 7.0 using sodium dithionite as a reductant, it was not possible to look for cytochrome c_1 species with extremely negative E_m values. Titrations, utilizing absorbance differences between several wavelength pairs in both the α- and Soret-band regions to monitor the heme redox state of cytochrome c_1, designed to measure the E_m value(s) for any cytochrome c_1 component(s) that might become reduced over the E_h range from +120 to −250 mV were unsuccessful. Thus, the E_m value(s) for possible distinct form(s) of the F138A and F138V variants that are reducible by dithionite but not by ascorbate remain, if such forms do indeed exist, remain to be elucidated.

Titrations of cytochrome bc_1 complexes containing four region 2 variants reveal that all four of these cytochrome c_1 variants, even one with a triple charge-reversal alteration (D189K/D190K/D196K), had E_m values for cytochrome c_1 that are essentially identical to that found for the wild-type cytochrome (Table 4). Given the effects, described above, of replacing Phe138 of *Rb. capsulatus* cytochrome c_1 with either alanine or valine on the E_m of the cytochrome, it is of particular interest that a similar set of replacements of the conserved aromatic residue, Tyr194, in region 2 of cytochrome c_1 had no effect on the E_m value of the cytochrome.

EPR Spectra. EPR spectra of ferricyanide-oxidized and ascorbate-reduced *Rb. capsulatus* cytochrome bc_1 complexes containing the F138Y, F138V, and F138A variants of cytochrome c_1, in the region of the low-field resonances associated with low-spin ferric hemes, are compared in Figure 4. The EPR properties of the F138Y variant are almost identical to those of the wild-type cytochrome bc_1 complex (*40*, *45*), with the $g = 3.79$ and 3.44 components attributed to cytochromes b_L and b_H, respectively; the ascorbate-reducible $g \sim 3.2$ component attributed to the native form of cytochrome c_1, with His/Met axial ligation; and the $g = 2.95$ component attributed to denatured bis-histidine *b*-type and/or c_1-type cytochromes. Thus, the EPR results (like the optical absorption and redox studies) indicate that heme prosthetic group of cytochrome c_1 is not significantly perturbed by the F138Y mutation.

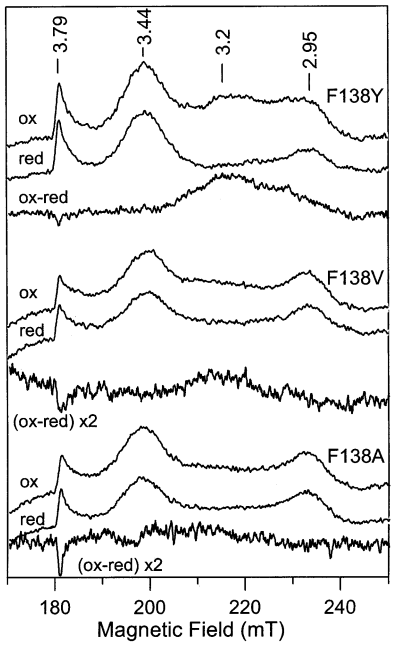

FIGURE 4: EPR spectra of ferricyanide-oxidized and ascorbate-reduced *Rb. capsulatus* cytochrome bc_1 complexes containing the F138Y, F138V, and F138A variants of cytochrome c_1, in the region of the low-field component of the low-spin ferric heme resonances. The sample concentrations were 136 μM (F138Y), 100 μM (F138V), and 118 μM (F138A). All samples were in 25 mM Tris-HCl buffer, pH 8.0, containing 10 mM NaCl and 0.01% dodecyl maltoside, and were oxidized with an equimolar amount of potassium ferricyanide or reduced with a 10-fold excess of sodium ascorbate. EPR spectra were recorded at 10 K, and the instrument settings were microwave frequency, 9.603 GHz; microwave power, 10 mW; and modulation amplitude, 6.4 G. The ferricyanide-oxidized minus ascorbate-reduced difference spectrum is shown directly under each pair of oxidized and reduced spectra.

Somewhat surprisingly, given the fact that the α- and β-band spectra of the F138V and F138A variants indicate that significant portions of these two cytochrome c_1 variants are reducible by ascorbate and are likely to be low-spin, no $g \sim 3.2$ EPR resonances characteristic of an ascorbate-reducible, low-spin ferric cytochrome c_1 with His/Met axial ligation were immediately apparent in the spectra of either the F138V or the F138A variants (see Figure 4). This was not a consequence of incomplete oxidation arising from the fact that a stoichiometric amount of ferricyanide was used to obtain the spectra of Figure 4, as the same result was observed for samples oxidized with a 10-fold excess of ferricyanide. However, for both variants, more detailed analysis involving the use of spectral subtractions of the ferricyanide-oxidized and ascorbate-reduced samples do reveal broad ascorbate-reducible components centered near $g = 3.2$ that can be attributed to the His/Met form of cytochrome c_1, on the basis of EPR and near-IR variable-temperature magnetic CD studies of the purified samples of wild-type eukaryotic and bacterial cytochrome c_1 proteins (*40*, *45*). The breadth and low amplitudes of these low-spin resonances in the F138A and F138V variants precluded reliable spin quantitation and may reflect greater heterogeneity than in wild-type cytochrome c_1 or the F138Y variant.

We also recorded EPR spectra over a wider spectral range to assess the possibility that a substantial portion of the c_1 cytochromes in the oxidized cytochrome bc_1 complexes containing the F138A and F138V mutations were in the high-

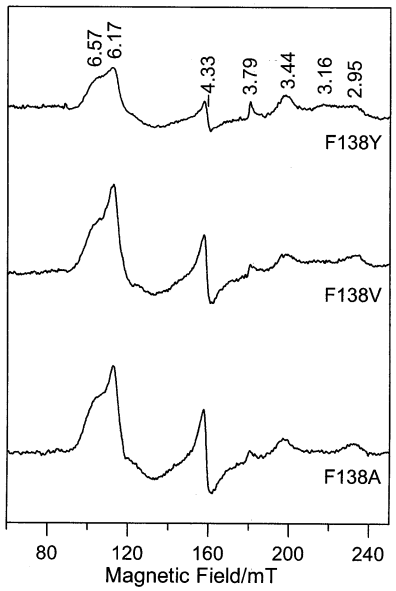

FIGURE 5: EPR spectra of ferricyanide-oxidized *Rb. capasulatus* cytochrome bc_1 complexes containing the F138Y, F138V, and F138A variants of cytochrome c_1 in the region of the low-field components of both the low-spin and the high-spin ferric heme resonances. The samples and measurement conditions are the same as those given in Figure 4.

spin state. As shown in Figure 5, the EPR spectra of oxidized samples of cytochrome bc_1 complexes containing the F138A and F138V variants of cytochrome c_1 do show more intense high-spin cytochrome signals in the $g = 6$ region, relative to the magnitude of the resonances from the *b*-type cytochromes at $g = 3.79$ and 3.44, than complexes containing the wild-type cytochrome or its F138Y variant (see Figure 5). The high-spin resonance comprises two overlapping resonances and was simulated as the sum of a near-axial component accounting for 20% of the high-spin resonance ($E/D = 0.001$, with effective *g*-values of 6.02, 5.98, and 2.00 for the lowest doublet) and a more rhombic component accounting for 80% of the high-spin resonance ($E/D = 0.024$, with effective *g*-values of 6.56, 5.42, and 1.98). However, quantitation of the simulated high-spin signals versus the $S = 1/2$ resonance of the reduced Rieske center in the same samples after reduction with dithionite revealed that the total high-spin heme component accounts for 0.03 spins in the F138Y variant and for 0.06 spins in the F138A and F138V variants. The magnitude of these high-spin signals did not decrease when the samples were reduced by ascorbate but did disappear when the samples were reduced with dithionite, indicating that the species that give rise to these signals are likely to have E_m values below +100 mV. However, the spin quantitations indicate that significant conversion of high-potential, ascorbate-reducible, low-spin ferric heme components with His/Met axial ligation to low-potential (i.e., not reducible by ascorbate) high-spin ferric heme components has not occurred and consequently cannot be responsible for the anomalies in α-band difference spectra discussed above.

Steady-State DBH_2/Cytochrome c Kinetic Parameters. Region 2 Variants. Equine cytochrome *c* and *Rb. capsulatus* cytochrome c_2 have similar tertiary structures, and both the V_{max} and K_m values for the two soluble cytochromes are virtually identical in the electron-transfer reaction from DBH_2 to cytochrome *c* that is catalyzed by the *Rb. capsulatus* cytochrome bc_1 complex (*20*). For this reason, and because of its ready availability, equine cytochrome *c* was used as the electron acceptor in steady-state activity measurements. All of the *Rb. capsulatus* cytochrome bc_1 complexes containing region 2 variants of cytochrome c_1 with charge-altering mutations, except for the D189E/D190E/D196E and D189K/D190K/D196K triple mutations, show V_{max} values for the DBH_2/cytochrome *c* oxidoreductase reaction that are at least 60% of that obtained with the cytochrome bc_1 complex containing wild-type cytochrome c_1 (Tables 3 and 4). Similar, relatively small, decreases in V_{max} had been observed previously for *Rb. sphaeroides* cytochrome bc_1 complexes containing region 2 variants of cytochrome c_1 (*23*). The magnitude of the modest decreases in V_{max} that occur when mutations are made at positions 189, 195, or 196 in *Rb. capsulatus* cytochrome c_1 are little effected by the identity of the replacement residue, over the limited range of substitutions explored in this study (Tables 3 and 4). When compared with modest decreases in V_{max} observed for cytochrome bc_1 complexes containing either the D189N/D190N or the D189N/D190N/D196N variants of cytochrome c_1, the somewhat larger decrease in V_{max} of the two other variants that contain three amino acid replacements (D189E/D190E/D196E and D189K/D190K/D196K) may perhaps reflect some nonspecific structural changes caused by introducing mutually repulsive residues within a small region of the protein. The possible presence of such a complicating secondary effect is illustrated by the D189E/D190E/D196E variant, as substitution of one negatively charged residue (aspartate) by another (glutamate) would not be expected to produce a large change in either V_{max} or K_m.

Changes in the K_m for cytochrome *c*, as compared with the K_m measured using the cytochrome bc_1 complex containing wild-type cytochrome c_1, of region 2 variants were also modest, as the largest K_m increase (i.e., that for the cytochrome bc_1 complex containing the D189K/D190K/D196K variant of cytochrome c_1) is only ca. 3-fold (Table 3). As replacing wild-type cytochrome c_1 by its D196K variant has almost no effect on the K_m value for cytochrome *c*, it can be inferred that the increase in K_m observed for the D189K/D190K/D196K variant is due to the mutations at either position 189 or 190 or both. The other charge elimination mutations in this region produced even smaller changes in K_m values (Table 3). Cytochrome bc_1 complexes containing alterations of cytochrome c_1 at the conserved region 2 aromatic residue Tyr194 (i.e., the Y194A, Y194V, and Y194F variants) exhibit K_m values that are almost identical to those observed for the complex containing wild-type cytochrome c_1 (Table 3). The V_{max} values measured for complexes containing position 194 variants of cytochrome c_1 are only slightly lower than that measured for the complex containing wild-type cytochrome c_1 (Tables 3 and 4). In sum, these results suggest that the region 2 acidic residues of *Rb. capsulatus* cytochrome c_1 are unlikely to be involved in the binding of cytochrome c_2 and that the conserved Tyr194 does not play any role in the electron-transfer reaction catalyzed by the *Rb. capsulatus* cytochrome bc_1 complex.

Phe138 Variants. Replacing Phe138 of *Rb. capsulatus* cytochrome c_1 by either alanine, valine, and to a lesser extent, tyrosine affected the V_{max} for the DBH_2/cytochrome *c* oxidoreductase activity of cytochrome bc_1 complexes containing the cytochrome c_1 variants (Tables 3 and 4). Purified

cytochrome bc_1 complexes containing either the F138V variant or the F138A variant of cytochrome c_1 retain only 50 and 16%, respectively, of the activity exhibited by a wild-type cytochrome bc_1 complex (Tables 3 and 4). Even replacement of Phe138 by another aromatic residue, tyrosine, produces a complex with a V_{max} only 55% of that observed for the complex containing wild-type cytochrome c_1 (Tables 3 and 4). In contrast to the effects on V_{max}, K_m values measured for cytochrome *c* with complexes containing these three position 138 variants are all quite similar to those measured for the complex containing wild-type cytochrome c_1 (Table 3).

To investigate whether these effects of position 138 substitutions on steady-state V_{max} values may have resulted from some effect on the stability of the complex during isolation and purification, the DBH_2/cytochrome *c* activities of complexes containing these variants were investigated using chromatophore membranes containing the complexes instead of detergent-solubilized, purified cytochrome bc_1 complexes (Table 4). Chromatophore activities were measured at an equine cytochrome *c* concentration of 100 μM, a value approximately 20-fold higher than the K_m measured for the purified cytochrome bc_1 complex containing wild-type cytochrome c_1 (Table 3), and thus are likely to reflect V_{max} values. Qualitatively, the results obtained with chromatophores containing the F138A or F138V variants of cytochrome c_1 are very similar to those measured for purified cytochrome bc_1 complexes (Table 4). The largest difference between relative steady-state activities measured with chromatophores and purified cytochrome bc_1 complexes was observed for the F138Y variant of cytochrome c_1, where a higher activity was observed with chromatophores (86% of the wild-type control) than with purified cytochrome bc_1 complexes (55% of the wild-type control). Despite this relatively small difference in activity of the purified cytochrome bc_1 complex as compared to activity in chromatophores observed for the F138Y variant, it appears that the loss in steady-state activity observed for the cytochrome bc_1 complexes containing either the F138V or the F138A variant of cytochrome c_1 cannot be attributed to loss of activity caused by detergent solubilization of the complex or its purification.

Flash-Induced Turnover Kinetics. The functional properties of cytochrome c_1 variants mutated at position 138 were also examined by monitoring flash-induced electron transfer in chromatophores. The presence of the cytochrome bc_1 complex, the membrane-anchored cytochrome c_y, the reaction center in chromatophore membranes, and the ability of cytochrome c_2 (trapped inside the chromatophores) to serve as a mobile electron carrier between the two membrane-bound complexes allows initiation of the catalytic cycle of the cytochrome bc_1 complex by transient triggering through the light-activated reaction center. Figure 6 shows the kinetics of cytochrome *c* rereduction (monitored at 550 nm minus 540 nm after an initial light-induced oxidation) in chromatophores containing either wild-type cytochrome c_1 (Figure 6A) or its F138A variant (Figure 6B). Kinetics were measured both in the absence of any inhibitor (black traces) and in the presence of stigmatellin, a specific inhibitor of the hydroquinone-oxidizing (Q_o) site of the cytochrome bc_1 complex (gray traces). Both the wild-type and the F138A samples show comparable kinetic behavior (i.e., efficient cytochrome *c* rereduction in the uninhibited state (Figure 6, black traces)) that is eliminated by addition of stigmatellin (Figure 6, gray traces). Chromatophores containing either the F138V or the F138Y variants of cytochrome c_1 also displayed similar kinetic behavior (not shown).

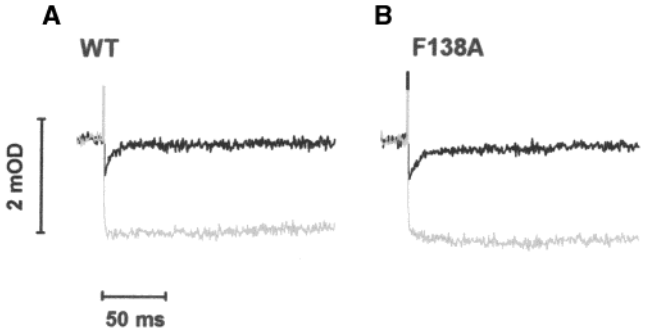

FIGURE 6: Flash-induced turnover kinetics of chromatophores containing mutated cytochrome c_1. Transient kinetics of the flash-induced oxidation and rereduction of cytochrome *c* were followed at 550−540 nm in chromatophores containing either wild-type cytochrome c_1 (A) or its F138A variant (B). The traces were obtained for samples poised at $E_h = +100$ mV (pH 7.0) either in the absence of inhibitor (black) or in the presence of 1 μM stigmatellin (gray).

The magnitudes of the differences between the total amplitude of the noninhibited and stigmatellin-inhibited traces are essentially identical for the wild-type and F138A samples, indicating that the fast, unresolved (on the ms time scale used for these measurements) phase of cytochrome *c* reduction characteristic of the wild type is also present in the F138A variant. This phase is now attributed to the movement of the Rieske subunit from the Q_o site to a position close to cytochrome c_1, followed by electron transfer from the [2Fe−2S] cluster of the Rieske protein to the heme of cytochrome c_1 (*3*). The data indicate that in freshly prepared chromatophore membranes, at least a significant portion of the cytochrome bc_1 complexes in which Phe138 has been replaced by alanine retains the efficient electron transfer through the high-potential chain of the cytochrome bc_1 complex that is characteristic of the wild-type complex.

DISCUSSION

The original impetus for this study was to explore the possibility that negatively charged amino acid residues in region 2 of *Rb. capsulatus* cytochrome c_1 and/or a conserved aromatic residue in this region were directly involved in the interaction of cytochrome c_1 with its electron-accepting partner cytochrome c/c_2. Although a mutagenesis study of the very similar *Rb. sphaeroides* cytochrome c_1 suggested that region 2 was not involved in binding cytochrome c/c_2 (*23*), the recently available structure for the complex between the yeast cytochrome bc_1 complex and its electron-accepting partner, cytochrome *c*, indicated that region 2 of yeast cytochrome c_1 was in fact involved in binding cytochrome *c* (*24*). The structure for the yeast complex is consistent with the earlier cross-linking data from the bovine system that implicated region 2 of cytochrome c_1 in binding cytochrome *c* (*22*). Given that cytochrome c/c_2 binding to detergent-solubilized cytochrome bc_1 complexes generally decreases greatly as the ionic strength increases (*15*, *20*, and references therein), indicating an important contribution from electrostatic interactions, it is perhaps surprising that most of the

contacts between yeast cytochromes *c* and c_1 in the crystal structure involve hydrophobic interactions between nonpolar amino acid side chains (*24*). Although the interaction between yeast cytochromes c_1 and *c* does involve one charged amino acid on cytochrome c_1 (i.e., E235), the corresponding residue in *Rb. capsulatus* cytochrome c_1, T193, is uncharged. Hydrophobic interactions between membrane-associated electron-transfer complexes in photosynthetic organisms and their soluble electron-transfer protein partners are known to be important in other systems, including the interaction between HiPIP (high-potential iron protein) and the reaction center in the photosynthetic purple non-sulfur bacterium *Rubrivivax gelatinosus* (*46*) and the interaction between plastocyanin and Photosystem 1 in oxygenic photosynthetic organisms (*47*).

The data obtained in this work indicate that site-specific mutations of acidic and aromatic residues in region 2 of *Rb. capsulatus* cytochrome c_1 have no significant effect on the redox properties of the cytochrome and very little effect on the activity of the cytochrome bc_1 complex. It is worth mentioning that the redox data obtained with the charge elimination and charge reversal mutations of acidic residues in region 2 (in some cases double and triple mutations) are consistent with the idea that individual surface charges do not, in general, significantly influence E_m values of redox proteins. In contrast, replacement of the conserved aromatic residue F138 in region 3 of *Rb. capsulatus* cytochrome c_1 by nonaromatic amino acids produced major changes in the oxidation−reduction and effects on the kinetic properties of the cytochrome bc_1 complexes containing these variants of cytochrome c_1 that were larger than those produced by changes in region 2 amino acids. In particular, the effects seen with F138 substitutions contrast with the very minor effects on steady-state activity, on spectroscopic, and on redox properties that arise from substitution at another highly conserved aromatic residue, Y194.

The most puzzling aspect of the data obtained with cytochrome bc_1 complexes containing the F138A and F138V variants of cytochrome c_1 is the fact that a substantial portion of the cytochrome no longer is ascorbate-reducible (but can be reduced by dithionite), despite the fact that the single component of each of these cytochrome c_1 variants detected in oxidation−reduction titrations each exhibited an E_m value (+220 mV for F138A and +245 mV for F138V) that is considerably more positive than that of the ascorbate/dehydroascorbate couple (E_m = +60 mV at pH 7.0). Given the possibility that the cytochrome c_1 heme in these two variants might have been slow to react with ascorbate, one might perhaps have attributed this observation to the fortuitous lowering of the E_m value for each of these variants (as compared to the E_m value for the wild-type cytochrome) to a point where a homogeneous population of each variant of the cytochrome was only partially reduced by ascorbate over the relatively short incubation times used to obtain the difference spectra obtained in this study. However, the observation that the magnitudes of α-bands for the single components of the F138A and F138V variants detected in redox titrations (carried out in the presence of redox mediators) are also considerably smaller than those measured for the wild-type cytochrome and its F138Y variant suggests that either the F138A and the F138V variants have smaller reduced minus oxidized extinction coefficients than the wild-type cytochrome or its F138Y variant or that these variants exhibit redox heterogeneity, with the component detected in the F138A and F138V redox titrations of Figure 3 accounting for only a portion of the cytochrome. The observation that the EPR spectra of the low-spin forms of the F138A and F138V variants of cytochrome c_1 are broader than those of the wild-type cytochrome and its F138Y variant, indicating greater heterogeneity in the F138A and F138V variants, is consistent with the possibility of lower α-band extinction coefficients for these variants. However, the fact that the magnitudes of the α-bands seen in dithionite minus ferricyanide difference spectra are almost identical for the wild-type cytochrome and its F138A, F138V, and F138Y variants appears to be more consistent with the existence of significant redox heterogeneity in the F138A and F138V variants. The very small amounts of high-spin cytochrome present in these two variants may contribute to small differences in the magnitudes of the α-bands seen in dithionite minus ferricyanide difference spectra but cannot contribute to the differences seen in ascorbate minus ferricyanide difference spectra because they are not reducible by ascorbate. Although only a single E_m component was detected in redox titrations of both the F138A and the F138V variants of cytochrome c_1, it is possible that a second component does exist but escaped detection because spectral overlap with absorbance changes arising from the *b*-type cytochromes masked this cytochrome c_1 component.

The results of flash-induced electron-transfer kinetics measured using purified chromatophores indicate that electron transfer within the high-potential chain of the cytochrome bc_1 complex is not affected by mutations at position F138 of cytochrome c_1, despite the fact that an approximately 100 mV decrease in the E_m value for a portion of cytochrome c_1 is observed for the F138V and F138A variants and the possibility that even larger decreases in E_m may occur for an additional portion of the mutated cytochrome in these two variants (i.e., the portion that is reduced by dithionite but not by ascorbate). This decrease in E_m of cytochrome c_1 would be expected to render the reduction of cytochrome c_1 by the Rieske iron−sulfur protein (E_m = +320 mV) thermodynamically less favorable in the F138V and F138A variants than is the case in the native cytochrome bc_1 complex, where the Rieske protein and cytochrome c_1 are approximately isopotential (*9*). Apparently, the occurrence of one such uphill electron-transfer step does not impair the overall operation of the high-potential portion of the cytochrome bc_1 complex, as long as the overall electron transfer process is thermodynamically favorable. Conceivably, the oxidizing power of the other high-potential components of the electron-transfer chain (P870 and cytochrome c_2/c_y) allows efficient electron transfer in the physiological direction to occur despite the presence of a thermodynamically unfavorable step (the decrease in the E_m value of cytochrome c_1 in the F138A and F138V variants will make electron transfer from cytochrome c_1 to the downstream acceptors cytochromes c_2 and c_y and $P870^+$ more favorable than is the case for wild-type cytochrome c_1). Similar situations have been encountered previously for revertants of *Rb. capsulatus* cytochrome c_1 variants in which the Cys144/Cys167 disulfide has been eliminated (*38*) and for variants of the *Rb. capsulatus* Rieske iron−sulfur protein (*48*), where mutations that change the E_m value for the mutated component by approximately 100 mV do not significantly impair electron

transfer through the high-potential chain of the cytochrome bc_1 complex. An alternation of thermodynamically favorable and thermodynamically unfavorable electron-transfer steps also seems to be a natural part of the electron-transfer mechanism within the tetraheme subunit of several bacterial reactions centers (*49*−*52*).

Recent X-ray diffraction studies of the *Rb. capsulatus* cytochrome bc_1 complex indicate that the aromatic side chain of F138 is too far from the heme of cytochrome c_1 (i.e., almost 6 Å) to be involved directly in electron transfer between the hemes of cytochromes c_1 and *c* (E. Berry, personal communication). However, the location of F138 in the structure of *Rb. capsulatus* cytochrome c_1 and the results reported above suggest that F138 may play an important role in maintaining the native structure around the heme domain of cytochrome c_1, a structure that is required to maintain the physicochemical properties associated with optimal electron transfer. Alterations in heme environment and properties resulting from replacement of a conserved aromatic residue are known to occur in other *c*-type cytochromes. One well-documented example involves peptide chain refolding when the conserved phenylalanine at position 82 of yeast iso-1-cytochrome *c* is replaced by nonaromatic amino acids (*53*). Replacement of F82 by either glycine or serine in the yeast cytochrome produces a decrease in heme E_m that arises from either changes in solvent accessibility or local polarity, and similar effects may be responsible for the ca. 100 mV decrease in the E_m value for *Rb. capsulatus* cytochrome c_1 that is observed when F138 is replaced by a smaller, nonaromatic residue. The hypothesis that an aromatic side chain is required at position 138 is supported by the observation that replacing F138 by another aromatic amino acid (i.e., tyrosine) produces a protein with properties very similar to those of wild-type *Rb. capsulatus* cytochrome c_1, while replacement of the aromatic side chain by an aliphatic one produces cytochrome c_1 variants that display altered EPR spectra, significantly less positive E_m values, and both redox and spin-state heterogeneity. The observation that replacing F138 by alanine has a greater effect on the properties of *Rb. capsulatus* cytochrome c_1 than is the case when F138 is replaced by valine may perhaps be due to the fact that the 64 $Å^3$ volume of the side chain of valine is closer to that of phenylalanine (93 $Å^3$), than is the case for the smaller (i.e., 26 $Å^3$) side chain of alanine (*54*).

In summary, this work provides new supporting evidence for the hypothesis, first proposed on the basis of mutagenesis studies of *Rb. sphaeroides* cytochrome c_1 (*23*), that negatively charged residues located in region 2 of cytochrome c_1 are not critical for physiologically important interactions between *Rb. capsulatus* cytochrome c_1 and its electron acceptors. This work also provides the first evidence that a conserved aromatic residue in region 2, Y194, is not directly involved in electron transfer between cytochrome c_1 and its electron acceptors. Moreover, new evidence has been obtained for a previously unsuspected critical role for an aromatic residue at position 138 of *Rb. capsulatus* cytochrome c_1 in maintaining the native environment around the heme cofactor of the cytochrome. Future analyses of additional mutations in this region of cytochrome c_1 will undoubtedly allow more detailed elucidation of the structural parameters essential for the efficient electron transfer by this component of the cytochrome bc_1 complex.

ACKNOWLEDGMENT

The authors would like to thank Drs. Edward Berry, Alain Desbois, and Francis Millett for helpful discussions.

REFERENCES

1. Yu, C. A., Tian, H., Zhang, L., Deng, K. P., Shenoy, S. K., Yu, L., Xia, D., Kim, H., and Deisenhofer, J. (1999) *J. Bioenerg. Biomembr. 31*, 191−199.
2. Berry, E. A., Guergova-Kuras, M., Huang, L. S., and Crofts, A. R. (2000) *Annu. Rev. Biochem. 69*, 1005−1075.
3. Darrouzet, E., Moser, C. C., Dutton, P. L., and Daldal, F. (2001) *Trends Biochem. Res. 26*, 445−451.
4. Gennis, R. B., Barquera, B., Hacker, B., Van Doren, S. R., Arnaud, S., Crofts, A. R., Davidson, E., Gray, K. A., and Daldal, F. (1993) *J. Bioenerg. Biomembr. 25*, 195−209.
5. Xia, D., Yu, C. A., Kim, H., Xia, J. Z., Kachurin, A. M., Zhang, L., Yu, L., and Deisenhofer, J. (1997) *Science 277*, 60−66.
6. Iwata, S., Lee, J. W., Okada, K., Lee, J. K., Iwata, M., Rasmussen, B., Link, T. A., Ramaswamy, S., and Jap, B. K. (1998) *Science 281*, 64−71.
7. Zhang, Z., Huang, L., Shulmeister, V. M., Chi, Y. I., Kim, K. K., Hung, L. W., Crofts, A. R., Berry, E. A., and Kim, S. H. (1998) *Nature 392*, 677−684.
8. Hunte, C., Koepke, J., Lange, C., Robmanith, T., and Michel, C. (2000) *Structure 8*, 669−684.
9. Gray, K. A., and Daldal, F. (1995) in *Anoxygenic Photosynthetic Bacteria* (Bauer, C. E., Ed.) pp 747−774, Kluwer Academic Publishers, Dordrecht, The Netherlands.
10. Yu, C. A., Zhang, L., Deng, K. P., Tian, H., Xia, D., Kim, H., Deisenhofer, J., and Yu, L. (1999) *Biofactors 9*, 103−109.
11. Brandt, U., and Trumpower, B. (1994) *Crit. Rev. Biochem. Mol. Biol. 29*, 165−197.
12. Daldal, F., Mandaci, S., Winterstein, C., Myllykallio, H., Duyck, K., and Zannoni, D. (2001) *J. Bacteriol. 183*, 2013−2024.
13. Menin, L., Schoepp, B., Parot, P., and Vermeglio, A. (1997) *Biochemistry 36*, 12183−12188.
14. Meyer, T. E., and Donohue, T. J. (1995) in *Anoxygenic Photosynthetic Bacteria* (Blankenship, R. E., Madigan, M. T., and Bauer, C. E., Eds.) pp 725−745, Kluwer Academic Publishers, Dordrecht, The Netherlands.
15. Bosshard, H. R., Wynn, R. M., and Knaff, D. B. (1987) *Biochemistry 26*, 7688−7693.
16. Hall, J., Kriauciunas, A., Knaff, D., and Millett, F. (1987) *J. Biol. Chem. 262*, 14005−14009.
17. Hall, J., Zha, X. H., Yu, L., Yu, C. A., and Millett, F. (1987) *Biochemistry 26*, 4501−4504.
18. Hall, J., Zha, X. H., Yu, L., Yu, C. A., and Millett, F. (1989) *Biochemistry 28*, 2568−2571.
19. Caffrey, M. S., and Cusanovich, M. A. (1991) *Arch. Biochem. Biophys. 285*, 227−230.
20. Guner, S., Willie, A., Millett, F., Caffrey, M. S., Cusanovich, M. A., Robertson, D. E., and Knaff, D. B. (1993) *Biochemistry 32*, 4793−4800.
21. Stonehuerner, J., O'Brien, P., Geren, L., Millett, F., Steidl, J., Yu, L., and Yu, C. A. (1985) *J. Biol. Chem. 260*, 5392−5398.
22. Broger, C., Salardi, S., and Azzi, A. (1983) *Eur. J. Biochem. 131*, 349−352.
23. Tian, H., Sadoski, R., Zhang, L., Yu, C. A., Yu, L., Durham, B., and Millett, F. (2000) *J. Biol. Chem. 275*, 9587−9595.
24. Lange, C., and Hunte, C. (2002) *Proc. Natl. Acad. Sci. U.S.A. 99*, 2800−2805.
25. Mauro, J. M., Fishel, L. A., Hazzard, J. T., Meyer, T. E., Tollin, G., Cusanovish, M. A., and Kraut, J. (1988) *Biochemistry 27*, 6243−6256.
26. Farchaus, J. W., Wachtveitl, J., Mathis, P., and Oesterhelt, D. (1993) *Biochemistry 32*, 10885−10893.
27. Wachtveitl, J., Farchaus, J. W., Mathis, P., and Oesterhelt, D. (1993) *Biochemistry 32*, 10894−10904.
28. Bruel, C., di Rago, J. P., Slonimski, P. P., and Lemesle-Meunier, D. (1995) *J. Biol. Chem. 270*, 22321−22328.
29. Wang, K., Zhen, Y., Sadoski, R., Grinnell, S., Geren, L., Ferguson-Miller, S., Durham, B., and Millett, F. (1999) *J. Biol. Chem. 274*, 38042−38050.
30. Zhen, Y., Hoganson, C. W., Babcock, G. T., and Ferguson-Miller, S. (1999) *J. Biol. Chem. 274*, 38032−38041.

31. Ponamarev, M. V., Schlarb, B. G., Howe, C. J., Carrell, C. J., Smith, J. L., Bendall, D. S., and Cramer, W. A. (2000) *Biochemistry 39*, 5971−5976.
32. Atta-Asafo-Adjei, E., and Daldal, F. (1991) *Proc. Natl. Acad. Sci. U.S.A. 88*, 492−496.
33. Darrouzet, E., Mandaci, S., Li, J., Qin, H., Knaff, D. B., and Daldal, F. (1999) *Biochemistry 38*, 7908−7917.
34. Andrews, K. M., Crofts, A. R., and Gennis, R. B. (1990) *Biochemistry 29*, 2645−2651.
35. Berry, E. A., and Trumpower, B. L. (1987) *Anal. Biochem. 161*, 1−15.
36. Dutton, P. L. (1978) *Methods Enzymol. 54*, 411−435.
37. Berry, E. A., and Trumpower, B. L. (1985) *J. Biol. Chem. 260*, 2458−2467.
38. Osyczka, A., Dutton, P. L., Moser, C. C., Darrouzet, E., and Daldal, F. (2001) *Biochemistry 40*, 14547−14556.
39. Straley, S. C., Parson, W. W., Mauzerall, D. C., and Clayton, R. K. (1973) *Biochim. Biophys. Acta 305*, 597−609.
40. Finnegan, M. G., Knaff, D. B., Qin, H., Gray, K. A., Daldal, F., Yu, L., Yu, C.-A., Kleis-SanFrancisco, S., and Johnson, M. K. (1996) *Biochim. Biophys. Acta 1274*, 9−20.
41. Aasa, R., and Vänngård, T. (1975) *J. Magn. Reson. 19*, 308−315.
42. Gray, K. A., Davidson, E., and Daldal, F. (1992) *Biochemistry 31*, 11864−11873.
43. Baymann, F., Robertson, D. E., Dutton, P. L., and Mantele, W. (1999) *Biochemistry 38*, 13188−13199.
44. Gray, K. A., Dutton, P. L., and Daldal, F. (1994) *Biochemistry 33*, 723−733.
45. Li, J., Darrouzet, E., Dhawan, I. K., Johnson, M. K., Osyczka, A., Daldal, F., and Knaff, D. B. (2002) *Biochim. Biophys. Acta 1556*, 175−186.
46. Osyczka, A., Nagashima, K. V. P., Sogabe, S., Miki, K., Shimada, K., and Matsuura, K. (1999) *Biochemistry 38*, 15779−15790.
47. Sigfridsson, K. (1998) *Photosynth. Res. 57*, 1−28.
48. Brasseur, G., Sled, V., Liebl, U., Ohnishi, T., and Daldal, F. (1997) *Biochemistry 36*, 11685−11696.
49. Nitschke, W., and Dracheva, S. M. (1995) in *Anoxygenic Photosynthetic Bacteria* (Blankenship, R. E., Madigan, M. T., and Bauer, C. E., Eds.) pp 775−805, Kluwer Academic Publishers, Dordrecht, The Netherlands.
50. Ortega, J. M., Drepper, F., and Mathis, P. (1999) *Photosynth. Res. 59*, 147−157.
51. Chen, I.-P., Mathis, P., Koepke, J., and Michel, H. (2000) *Biochemistry 39*, 3592−3602.
52. Rousset, M., Montet, Y., Guigliarelli, B., Forget, N., Asso, M., Bertrand, P., Fontecilla-Camps, J. C., and Hatchikian, E. C. (1998) *Proc. Natl. Acad. Sci. U.S.A. 95*, 11625−11630.
53. Louie, G. V., and Brayer, G. D. (1989) *J. Mol. Biol. 209*, 313−322.
54. Richards, F. M. (1974) *J. Mol. Biol. 82*, 1−14.

BI020693R